Chapter 13

Bimolecular Fluorescence Complementation to Assay the Interactions of Ubiquitylation Enzymes in Living Yeast Cells

Ewa Blaszczak, Claude Prigent, and Gwenaël Rabut

Abstract

Ubiquitylation is a versatile posttranslational protein modification catalyzed through the concerted action of ubiquitin-conjugating enzymes (E2s) and ubiquitin ligases (E3s). These enzymes form transient complexes with each other and their modification substrates and determine the nature of the ubiquitin signals attached to their substrates. One challenge in the field of protein ubiquitylation is thus to identify the E2–E3 pairs that function in the cell. In this chapter, we describe the use of bimolecular fluorescence complementation to assay E2–E3 interactions in living cells, using budding yeast as a model organism.

Key words Ubiquitin, Ubiquitin-conjugating enzyme, Ubiquitin ligase, Protein–protein interactions, Protein-fragment complementation assay, BiFC, Living cell, *Saccharomyces cerevisiae*, Microscopy, Linear unmixing

1 Introduction

Conjugation of the small protein ubiquitin to other cellular proteins, a process termed ubiquitylation, regulates the homeostasis and activity of thousands of proteins in eukaryotic cells [1–3]. It is achieved through a hierarchical network of enzymes that comprises ~30 ubiquitin-conjugating enzymes (E2s) and more than 600 known or putative ubiquitin ligases (E3s) in human cells [4, 5]. In this network, E2s carry activated ubiquitin, while E3s allow the transfer of ubiquitin from E2s to substrate proteins. E2s and E3s can also conjugate ubiquitin to ubiquitin moieties already attached to substrate proteins, which leads to the assembly of polymeric ubiquitin chains. In ubiquitin chains, any of the seven lysine residues of ubiquitin or its N-terminus can be modified by a subsequent ubiquitin. Substrate proteins can thus be modified by mono-ubiquitin moieties or by various types of poly-ubiquitin chains that can be complex and contain heterogeneous

Rune Matthiesen (ed.), *Proteostasis: Methods and Protocols*, Methods in Molecular Biology, vol. 1449,
DOI 10.1007/978-1-4939-3756-1_13,

ubiquitin-ubiquitin linkages [6]. It is now well established that the nature of the ubiquitin modification attached to a substrate protein encode distinct molecular signals that trigger different responses in the cell. Deciphering how this ubiquitin code is written by E2s and E3s and interpreted by the cell machinery is thus a central question in the field [7].

Structural and biochemical studies have revealed many details on the interaction and catalytic mechanism of individual E2s and E3s, but an important challenge is to understand how these enzymes operate at a network level in living cells. For instance, when investigating the activity of a given E3, it is critical to exhaustively describe the range of E2s that can function with this E3. This is not easily done, since we are currently not able to accurately predict which E2s and E3s can interact with each other and conventional biochemical methods such as immunoprecipitation often do not succeed to capture E2–E3 interactions due to their low affinity. Yeast two-hybrid approaches are able to detect weak interactions and have been used with some success to systematically assay the human E2–E3 interactome [8, 9]. However, these screens did not identify E2 partners for numerous E3s, which may in part be due to the fact that many E3s function as heterodimers or as large protein complexes that are not reconstituted in a yeast two-hybrid assay. For instance, E2 partners of the human BRCA1-BARD1 heterodimeric E3 complex could only be identified by yeast two-hybrid when using a bait construct consisting of the catalytic domains of BRCA1 and BARD1 fused in a single polypeptide that folds into a correct E3 structure [10]. To overcome this limitation, we recently introduced the use of bimolecular fluorescence complementation (BiFC) as a mean to assay E2–E3 interactions in their native cellular context [11]. BiFC is a protein-fragment complementation assay where two proteins of interest, here an E2 and an E3, are fused to complementary N- and C-terminal fragments of a fluorescent protein reporter (reviewed in [12–16]). Upon E2–E3 interaction, the fragments of the fluorescent protein are brought into close proximity, allowing them to fold and to reconstitute an active fluorescent protein, which can then be detected using fluorescence microscopy (Fig. 1).

In this chapter, we describe critical aspects on the design of BiFC experiments and present imaging conditions and image processing steps for sensitive detection and quantification of BiFC complex formation in budding yeast (protocols describing how to implement BiFC experiment in other model organisms have been described elsewhere, *see* for instance [17–19] and **Note 1**). The sensitivity of fluorescence microscopy experiments in yeast is limited by the background fluorescence (autofluorescence) of the cells that hinders the detection of weak fluorescence signals of interest. This is particularly an issue in BiFC experiments as only a fraction of the fusion proteins form BiFC complexes. The fluorescence

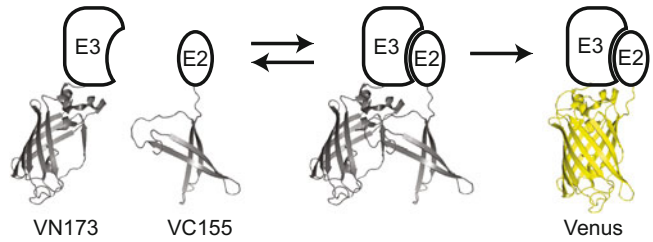

Fig. 1 *Principle of BiFC to image E2–E3 interactions*. E2s and E3s of interest are tagged with complementary fragments of a fluorescent protein (e.g., VN173 and VC155). Upon E2–E3 interaction, the fragments are brought in close proximity which allows irreversible reconstitution of the fluorescent protein (e.g. Venus)

intensities produced by BiFC complexes are thus typically less than 10% of the fluorescence intensity that would be produced by the corresponding proteins fused to an intact fluorescent protein [14]. In the method section, we therefore first describe how to cultivate yeast cells to minimize cell autofluorescence and how to setup imaging conditions to lower its contribution in the images. We then describe an image processing workflow to digitally subtract autofluorescence from BiFC images and quantify BiFC signals in single cells (Fig. 2). Overall this method enables sensitive visualization and quantification of E2–E3 interactions in budding yeast.

1.1 Critical Considerations and Design of BiFC Experiments in Yeast

1.1.1 Advantages and Limitations of BiFC

Excellent reviews have described in details the characteristics, advantages, and limitations of BiFC [12–16]. In addition to the ease with which it can be implemented, an important asset of BiFC over other methods used to monitor protein–protein interactions (PPIs) in living cells is its ability to detect very weak PPIs, with dissociation constants up to 1 mM [20, 21]. BiFC is thus perfectly suited to reveal E2–E3 interactions that have dissociation constants in the micromolar range [4]. This ability of BiFC to detect weak interactions originates from the fact that the reconstitution of a fluorescent protein from its complementary fragments is essentially irreversible (Fig. 1). This property has been documented in vitro and in vivo with several fluorescent proteins, including the widely used variant of the yellow fluorescent protein Venus (see [22] and references therein). BiFC thus acts as a trap that captures PPIs. Inevitably, it can also capture nonspecific protein–protein collisions that occur randomly in the cell, leading to false positive fluorescence. This caveat of BiFC is particularly problematical when proteins are highly expressed or locally concentrated as this leads to higher collision frequencies [23]. BiFC is therefore a valuable method to investigate E2–E3 interactions in the context of living cells, but adequate controls (see below) and independent assays are required to demonstrate that the detected interactions are indeed specific and biologically meaningful.

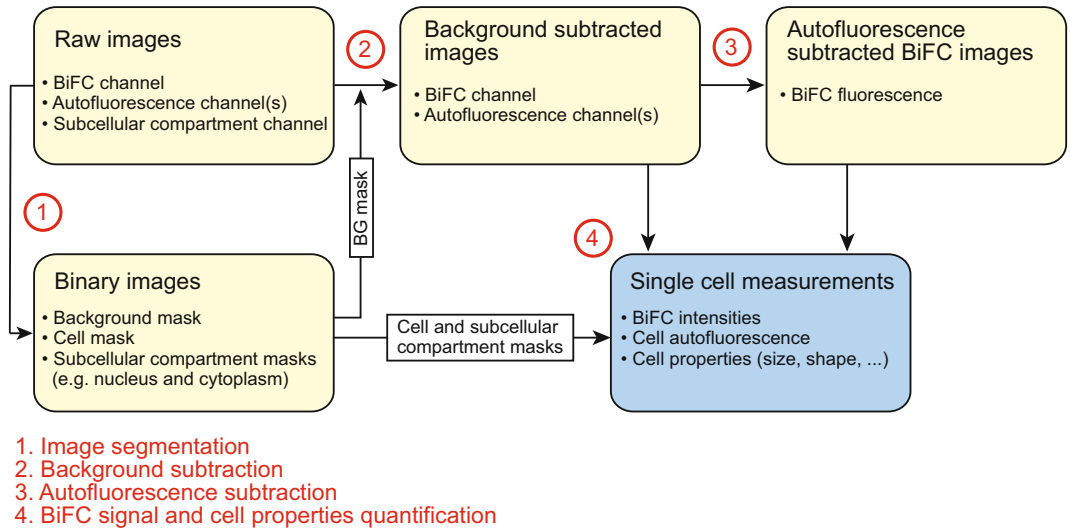

Fig. 2 *Scheme of the image processing workflow*. The image processing procedure described in this chapter involves four steps: Image segmentation (1), background subtraction (2), autofluorescence subtraction (3), and BiFC signal and cell property quantification (4). (1) Image segmentation produces binary images (*see* Fig. 3) that are then used in the subsequent image processing steps and for fluorescence quantification. (2) Background subtraction is performed using background mask produced during image segmentation. This step is required to be able to perform quantitative measurements of BiFC signals. (3) Autofluorescence subtraction reduces the contribution of autofluorescence in BiFC channel images, which improves the quality of the BiFC images (*see* Fig. 4) and the quantification of BiFC signals. (4) BiFC signal is quantified in single cells using the autofluorescence subtracted BiFC channel image and subcellular compartment masks. The quantification of other cell properties can also improve the analysis of BiFC signals. For instance, quantifying cell autofluorescence is useful to eliminate dead (strongly autofluorescent) cells, while measuring cell size can enable to distinguish bud and mother cells

Another limitation of BiFC is the slow maturation of fluorescent proteins. In budding yeast, the half-life of Venus maturation has been estimated to be ~15 min [24]. This creates a delay between the time when the fusion proteins interact with each other and the time when the complex actually becomes fluorescent. Both the delay and the irreversible nature of fluorescent protein reconstitution limit the use of BiFC to investigate temporal changes in E2–E3 interactions. Since interactions are not observed in real time, care should also be taken in the interpretation of fluorescence localizations. What is observed in BiFC images is the localization of trapped BiFC complexes, which may not always correspond to the site where the interaction of the two proteins takes place.

1.1.2 Choice of Fluorescent Protein Fragments

Numerous fluorescent proteins have been used in BiFC assays (reviewed in [15, 16]). In yeast as in other organisms, the Venus fluorescent protein is most widely used because its fragments produce the highest level of BiFC fluorescence [25]. It is commonly split at residues 173 and 155 to produce overlapping N-terminal

and C-terminal fragments (VN173 and VC155, respectively), yet other efficient fragment combinations have been described (see for instance [26, 27]). As aforementioned, Venus fragments are prone to self-assembly. Multiple attempts have been made to improve the specificity of Venus-based BiFC [22, 27–30], but many of the proposed solutions also reduce the intensity of specific BiFC fluorescence and have not been tested in yeast. As long as optimized fragments have not been clearly established in yeast, we suggest using the VN173 and VC155 fragments for which most tools are currently available. These tools notably include plasmids for one-step PCR-mediated fusion of endogenous genes with VN173 or VC155 [31] (these plasmids are available from the EUROSCARF, http://web.uni-frankfurt.de/fb15/mikro/euroscarf/data/Huh.html), but also a collection of 5809 VN173-tagged yeast strains that comprises most yeast E2s and E3s [32] (these strains are commercially available as single strains or as the whole collection from the Korean Biotech company Bioneer, http://eng.bioneer.com/products/YeastGenome/VN-FusionLibrary-overview.aspx). Note that it is possible to introduce the A206K mutation in VC155 to prevent dimerization of the reconstituted Venus protein [26].

1.1.3 Construction of Yeast Strains for BiFC Experiments

The design of the fusion proteins is an essential step in BiFC experiments. Clearly, the localization and interaction of the two protein partners should not be impaired by the fluorescent protein fragments. In addition, the fluorescent proteins fragments should be positioned in such a way that, upon interaction of the two partners, they can meet and reconstitute the reporter fluorescent protein. These criteria are often tested empirically by fusing the fragments to either end of the investigated proteins. Since many E3s are large multi-domain proteins, we suggest tagging them first at the end which is the closest to their catalytic domain (i.e. the C-terminus for most E3s). This should help to position the fluorescent protein fragment in proximity to any potential interacting E2. Note that tagging E3s may impair their catalytic activity without necessarily disturbing E2 interactions. For instance, C-terminal tags inactivate HECT E3s [33, 34] because they impair the positioning of residues of the E3 C-terminal tail that are involved in catalysis [35] but that do not participate in E2 recruitment [36, 37]. Yeast E2s are small proteins and may successfully be tagged at either end, with the exception of Ubc6 and Ubc7 that have to be tagged N-terminally (Ubc6 C-terminus contains a transmembrane domain and faces the lumen of the endoplasmic reticulum [38], while Ubc7 C-terminus is involved in the interaction with its partner Cue1 [39]).

While performing BiFC experiments in yeast, it is best to replace the endogenous genes with their tagged versions. This ensures that the tagged proteins are expressed at physiological concentrations and that there is no competition between the tagged and untagged proteins. Yet, we observed that several E2s

endogenously tagged with VC155 are significantly less expressed than the wild-type proteins (unpublished results). We have not examined the reason for this, but it may partly be due to poor folding of the VC155 fragment [14].

BiFC assays in yeast are particularly well suited for large scale analysis of PPIs. It is therefore advantageous to construct the E2 and E3 tagged strains in a genetic background compatible with high-throughput yeast manipulation. The strains we use carry the can1::STE2pr-spHIS5 and lyp1::STE3pr-HPH markers to allow automatic strain crossing and selection of the haploid progeny of either MATa or MATalpha mating type [11]. Protocols for high-throughput yeast manipulation have been described in details elsewhere [40]. In addition, we recommend including in the constructed strains a marker of a subcellular compartment fused to a red fluorescent protein (e.g., we used Rpn7-tDimer2 as a nuclear marker [11]). This enables to get precise information on the possible subcellular localization of the interaction, but also helps to achieve robust and sensitive measurements of BiFC fluorescence intensities.

1.1.4 Negative Controls

One of the challenges while performing BiFC experiments is the identification of appropriate negative controls to distinguish *bona fide* interactions from nonspecific self-assembly of the fluorescent protein fragments. Ideally, one should replace one of the two binding partners with a version mutated in its interaction surface [15]. The mutant protein should be fused to the fluorescent protein fragment in the same way as the wild-type protein and should display the same expression level and subcellular localization. Designing such mutants of E2s or E3s may not always be straightforward. In some instances, E3s engage multiple contacts with their E2s that involve not only the E3 catalytic domain, but also another region of the E3 or an auxiliary subunit [41]. In the case where E2 or E3 interaction mutants cannot be easily designed, it is possible to perform competition experiments by overexpressing an untagged version of one of the binding partners [15]. Importantly, the use of fluorescent protein fragments unfused, or fused to an irrelevant protein, is not a suitable negative control because the efficiency of non-specific self-assembly of fluorescent protein fragments is influenced by the nature of the proteins they are fused to [42]. In addition, such constructs are unlikely to be expressed at the same level and to have the same subcellular localization as the original fusion protein.

Importantly, the biological significance of specific PPIs identified by BiFC should be established using fully independent assays. BiFC may reveal indirect or enzyme-substrate interactions (see for instance [43]). Furthermore, some E2s and E3s can interact *via* their catalytic domains without triggering ubiquitylation (see for instance [10, 44]). E2–E3 interactions revealed by BiFC therefore need to be carefully characterized by independent in vivo and in vitro experiments to determine their nature and functional relevance.

2 Materials

2.1 Yeast Cultures

1. YPD plates: 1% (w/v) yeast extract, 2% (w/v) peptone, 2% (w/v) dextrose, 2% (w/v) agar in dH_2O. Autoclave at 121 °C for 15 min. Cool down to 55 °C before pouring the plates.
2. YPD + Ade medium: 1% (w/v) yeast extract, 2% (w/v) peptone, 2% (w/v) dextrose, 20 mg/L adenine hemisulfate in dH_2O. Autoclave at 121 °C for 15 min.
3. Sterile 14 mL round-bottom culture tubes or sterile U-shaped 2 mL 96-deepwell plates (to be sealed using sterile air-permeable sealing films for cell culture).

2.2 Microscopy

1. 10× Low-fluorescence nitrogen base: 5 g $(NH_4)_2SO_4$, 1 g KH_2PO_4, 0.5 g $MgSO_4$, 0.1 g NaCl, 0.1 g Ca_2Cl, 0.5 mg H_3BO_4, 0.04 mg $CuSO_4$, 0.1 mg KI, 0.2 mg $FeCl_3$, 0.4 mg $MnSO_4$, 0.2 mg Na_2MoO_4, 0.4 mg $ZnSO_4$, 2 μg biotin, 0.4 mg calcium pantothenate, 2 mg inositol, 0.4 mg niacin, 0.2 mg PABA, 0.4 mg pyridoxine HCl, 0.4 mg thiamine in 100 mL dH_2O. Autoclave at 121 °C.
2. 10× Amino acids: 20 mg Adenine hemisulfate, 20 mg Uracil, 20 mg L-Histidine HCl, 30 mg L-lysine HCl, 60 mg L-leucine, 20 mg L-methionine, 20 mg L-tryptophan in 100 mL dH_2O. Filter sterilize.
3. Low-fluorescence medium (LFM): 2 g Dextrose, 10 mL 10× low-fluorescence nitrogen base, 10 mL 10× amino acids in 100 mL dH_2O. Filter sterilize.
4. 8-Well coverglass imaging chambers (e.g., Nunc™ Lab-Tek™ II chambers, Thermo Scientific, USA) or 96-well coverglass imaging plates (e.g., Imaging Plates CG, ZellKontakt GmbH, Germany).
5. Inverted epifluorescence or confocal microscope equipped with suitable filters and objectives (*see* **Note 2** and Subheading 3). For high-throughput BiFC experiments, the microscope should be equipped with a XYZ motorized stage and a 96-well plate holder.

2.3 Image Processing

1. Image processing software (e.g., ImageJ, Fiji or CellProfiler).

3 Methods

3.1 Cell Preparation for Microscopy

1. *Day 1*: Inoculate YPD agar plates with the yeast strains of interest and incubate them overnight at 30 °C. Include positive, negative and no-BiFC control strains (*see* **Note 3**).
2. *Day 2, morning*: Inoculate 1 mL liquid YPD + Ade cultures at an OD_{600} of ~0.2 using the freshly grown cells (*see* **Note 4**).

Depending on the number of strains to analyze, the cultures can be grown in individual sterile 14 mL round-bottom tubes or U-shaped 2 mL 96-deepwell plates sealed with an air-permeable sealing. Cultivate under constant agitation at 25 °C in a shaking incubator (*see* **Note 5**).

3. *Day 2, evening*: Use 100 µL of each culture to measure their OD_{600} and dilute them to an OD_{600} of 0.001–0.005 in 1 mL YPD + Ade (*see* **Note 6**). Cultivate overnight under constant agitation at 25 °C in a shaking incubator.
4. *Day 3, morning*: Harvest the cells from the overnight cultures by centrifugation at 3000 × *g* for 3 min and resuspend them in 300 µL of liquid LFM medium prewarmed to 25 °C. Use 100 µL to measure the OD_{600} and use the rest of the cells to inoculate 0.5 mL LFM cultures at an OD_{600} of 0.3 in individual tubes or 96-deepwell plates. Incubate the cultures under agitation for at least 3 h at 25 °C (*see* **Note 7**).
5. *Day 3, afternoon*: Microscopy can be performed in 8-well coverglass chambers or 96 well coverglass plates, depending on the number of strains to analyze. For 8-well chambers, place 200 µL of each culture in the wells and then add in each well 300 µL of LFM medium prewarmed to 25 °C. For 96-well plates, place 80 µL of each culture in the wells and then add in each well 120 µL of prewarmed LFM medium. Let the cells settle to the bottom of the wells for 30 min before proceeding with imaging (*see* **Note 8**).

3.2 Image Acquisition

1. *Objective lens*: The choice of the objective is critical. To maximize the amount of fluorescence collected from the cells and obtain a good horizontal resolution, choose a high numerical aperture (NA) and high magnification objective. Avoid objectives designed for phase contrast and remove differential interference contrast phase plates and prisms from the optical path because they would significantly reduce transmission. Objectives with a correction collar are convenient to correct small variations in cover glass thickness and achieve maximum image quality. Note that when imaging yeast strains in 96-well plates it is more convenient to use water or glycerol rather than oil as the immersion medium. We use a Leica HC PL APO 63×/1.20 W motCORR CS2 objective.
2. *BiFC channel*: This channel collects the light emitted by BiFC complexes but also by cell autofluorescence. To lower the contribution of autofluorescence, design image acquisition settings that maximize the ratio of the light collected from BiFC fluorescence over autofluorescence. This is typically achieved using a narrow bandpass filter around the emission peak of the fluorescent protein. Excitation should also be performed using a narrow passband at the excitation peak of the fluorescent

protein. We typically use a 514 nm excitation laser and a 525–538 nm bandpass emission filter to image Venus BiFC (Venus excitation and emission peaks are 515 and 528 nm, respectively). The image acquisition settings need to be optimized for each microscope using positive and no-BiFC control strains (*see* **Note 3**).

3. *Autofluorescence channel(s)*: To be able to digitally subtract autofluorescence from BiFC channel images, it is necessary to record independent images of the cell autofluorescence. The image acquisition settings for those images should be designed to maximize the ratio of the light collected from autofluorescence over BiFC fluorescence (*see* **Note 9**). Excitation may be performed using a passband away from the excitation peak of the fluorescent protein. In addition, to achieve accurate autofluorescence subtraction, it can be beneficial to define several autofluorescence channels. In our experiments, we typically use two autofluorescence channels, acquired with 458 and 514 nm excitation lasers and 500–540 and 480–505 nm bandpass emission filters, respectively (*see* Fig. 4). Importantly, the primary autofluorescence channel will be used for segmentation of the cells (see below and Fig. 3). It should have a good signal-to-noise ratio and should enable to clearly recognize the contour of the cells.
4. *Subcellular compartment channel*: We recommend acquiring images of a subcellular compartment of interest stained with a protein marker fused to a red fluorescent protein. For instance, we routinely use Rpn7-tDimer2 as a nuclear marker (Fig. 3). We acquire these images simultaneously with the BiFC channel images using a 561 nm excitation laser and a 580–630 nm bandpass emission filter. These images need to have a sufficiently good signal to noise ratio to enable segmentation (see below).
5. *Confocal-specific settings:* Pixel size and pinhole diameter need to be carefully adjusted as these parameters strongly influences the quality of the images. Larger pixels yield brighter images with better signal-to-noise ratios. For sensitive quantification of weak BiFC signals, it is therefore beneficial to increase pixel size, even if this is at the cost of a reduced spatial resolution. We routinely use 0.25 mm wide pixels. Similarly, opening the pinhole allows more light to reach the photodetector and yields brighter images.

3.3 Image Processing and BiFC Signal Quantification

Image processing is used to digitally subtract autofluorescence from BiFC channel images and to produce quantitative BiFC measurements in single cells. The workflow of the image processing steps is schematized in Fig. 2. It can be automatized using macros or plug-ins in ImageJ and Fiji (*see* **Note 10**), or pipelines in CellProfiler.

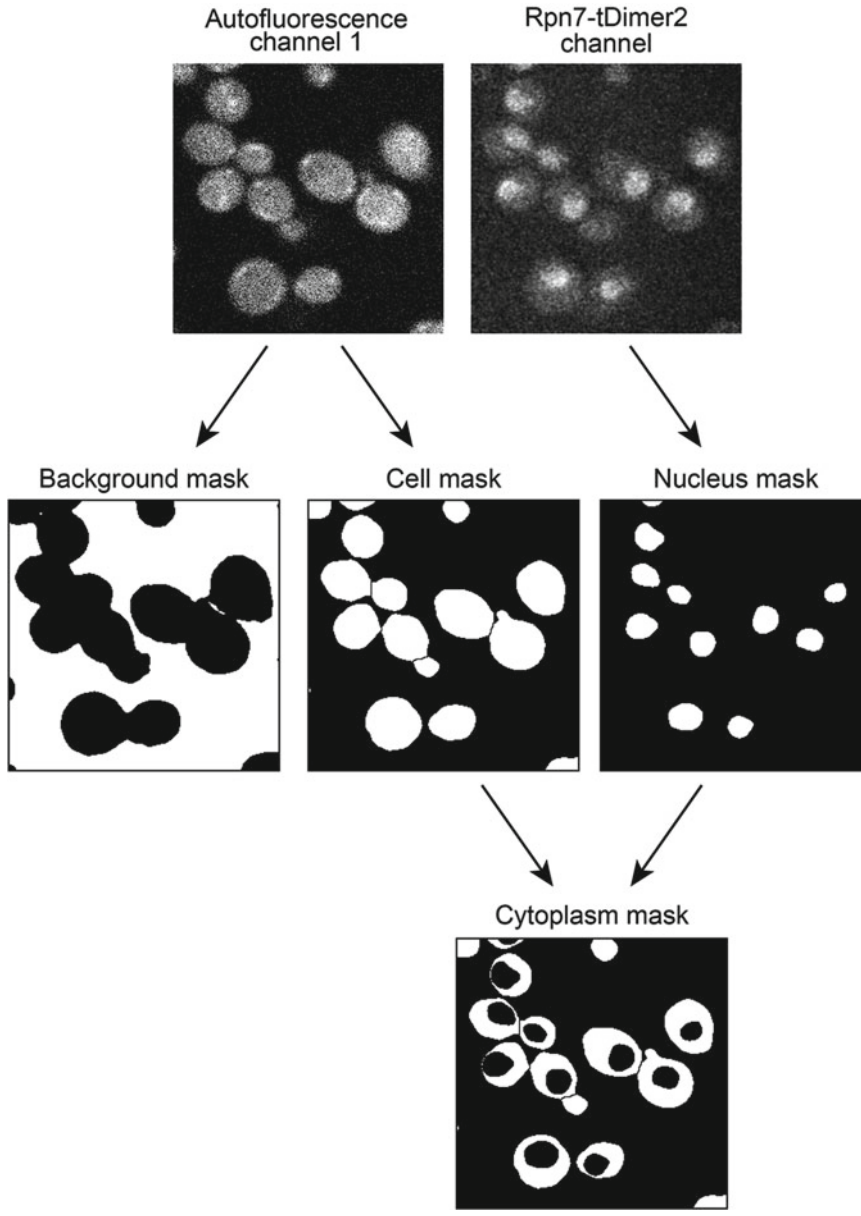

Fig. 3 *Image segmentation*. The image segmentation procedure described in this chapter uses the raw images acquired with the primary autofluorescence channel and with the subcellular compartment channel to produce four types of binary images. The autofluorescence image is first processed to select either the lower intensity pixels, which produces a binary image of the background pixels (background mask), or the higher-intensity pixels, which produces a binary image of the cell pixels (cell mask). Similarly, the subcellular compartment image (here Rpn7-tDimer2) is processed to select the higher-intensity pixels, which produces a binary image of the subcellular compartment pixels (e.g., nucleus mask). Combining this image with the cell mask enables to produce a binary image of the rest of the cell (e.g., cytoplasm mask)

Fig. 4 (continued) were cultivated and imaged as indicated in Subheading 3. The background subtracted BiFC and autofluorescence channel images are shown in the *left panel* and the BiFC images produced after autofluorescence subtraction are shown in the *right panel*. These images were then further processed using the PureDenoise Plugin for ImageJ [52] to reduce pixel noise and improve BiFC signal visualization. The interaction between VC155-Ubc6 and Asi3-VN173 (*top row*) produces a BiFC signal at the nuclear rim that can be easily detected in the background-subtracted image and that is improved after autofluorescence subtraction. In contrast, the interaction between VC155-Ubc6 and Asi1-VN173 (*bottom row*) produces a BiFC signal that is barely detectable without autofluorescence subtraction

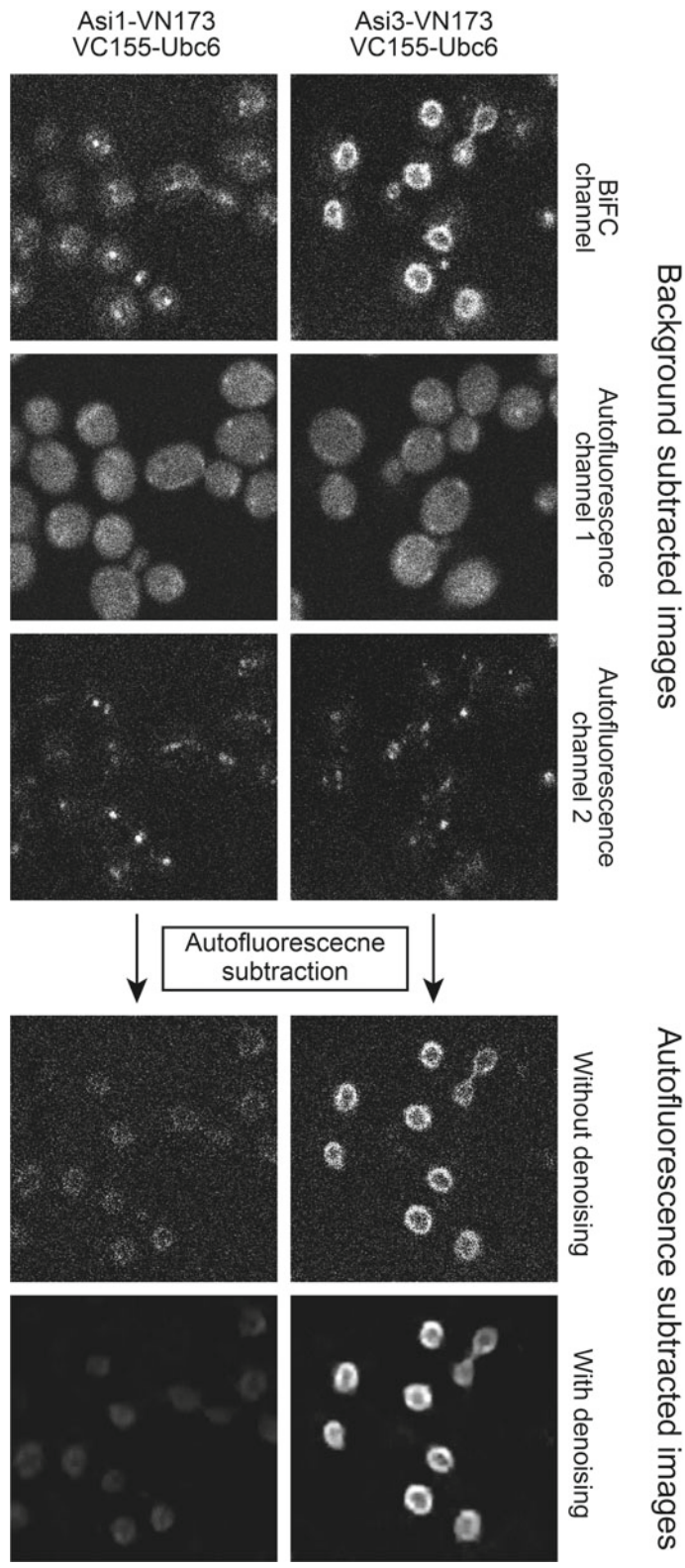

Fig. 4 *Autofluorescence subtraction improves the detection of weak BiFC signals*. This figure illustrates how autofluorescence subtraction enables to improve the quality of BiFC images and the detection of weak BiFC signals. Haploid yeast cells expressing the E2 Ubc6 tagged with VC (VC155-Ubc6) and the inner nuclear membrane localized E3s Asi3 or Asi1 tagged with VN (Asi3-VN173, *top row*, and Asi1-VN173, *bottom row*) from their endogenous chromosomal loci

3.3.1 Image Segmentation

The first step in image processing is segmentation. The procedure described here produces 4 binary images (*see* Fig. 3) that are then used to select the pixels to include in fluorescence measurements.

1. Open the image acquired with the primary autofluorescence channel.
2. Apply a spatial filter to remove pixel noise and small objects in this image (*see* **Note 11**). Duplicate the filtered image.
3. Threshold the filtered image: Set the lower threshold to the minimum pixel intensity of the image and adjust the upper threshold value to produce a binary image corresponding to background regions of the image field (*see* **Note 12**). The selected threshold value should be sufficiently low to ensure that the selected pixels do not contain any fluorescence from cell edges. Divide the resulting image with 255 (*see* **Note 13**). This step produces a binary mask that will be used to quantify background intensity (see below).
4. Threshold the duplicated filtered image: Set the upper threshold to the maximum pixel intensity of the image and adjust the lower threshold value to produce a binary image corresponding to the cells (*see* **Note 12**). The threshold value selected here should be higher than the threshold used in **step 3** and enable to nicely delineate the contour of individual cells.
5. *Optional step*: Improve the binary image produced in **step 4** by applying morphological operators. For instance, performing an erosion followed by dilation smooths objects and removes isolated pixels.
6. Apply a watershed transformation. This operation is essential to individualize cells that are touching each other and that could not be separated by thresholding. This step produces a binary image that will be used to identify individual cells for BiFC fluorescence quantification (see below).
7. Open the image acquired with the subcellular compartment channel. Apply a spatial filter as in **step 1**, threshold the filtered image as in **step 4** and, if necessary, improve the image as in **step 5**.
8. Divide the subcellular compartment binary image produced in **step 7** by 255 (*see* **Note 13**). This produces the binary mask that will be used to quantify fluorescence signals in this compartment (e.g., the nucleus) (see below).
9. Invert the subcellular compartment binary image produced in **step 7**, multiply it with the binary image produced in **step 6** and divide the resulting image by 255 (*see* **Note 13**). This produces the binary mask that will be used to quantify fluorescence signals in the rest of the cell (e.g., the cytoplasm) (see below).

3.3.2 Background Subtraction

Background must be subtracted from BiFC and autofluorescence channel images before further processing (*see* **Note 14**).

1. Open the image acquired with the BiFC channel. Convert it to a 32-bit float image (*see* **Note 15**).
2. Multiply the image with the background binary mask produced in **step 3** of image segmentation. This produces an image where all pixel values are set to zero except background pixels.
3. Measure the integrated density (i.e., the sum of all pixel values) in this image and divide it with the integrated density of the binary mask. This operation calculates the average intensity of background pixels.
4. Subtract the average background intensity from all pixel values in the BiFC channel image.
5. Repeat **steps 1–4** with the image(s) acquired with the autofluorescence channel(s).

3.3.3 Autofluorescence Subtraction

This step aims to remove autofluorescence signals from the BiFC channel image, which significantly improves the detection and quantification of weak BiFC signals (Fig. 4). To this end, the autofluorescence channel images are rescaled and subtracted from the BiFC channel images. The identification of a correct rescaling factor for each autofluorescence channel is done empirically using images of no-BiFC control cells (*see* **Note 3**). Once such factors have been identified, they can be applied to all other images acquired in identical conditions.

1. Open the background subtracted BiFC channel and autofluorescence channel images of no-BiFC control cells.
2. Multiply each autofluorescence channel image by a separate rescaling factor. The initial value of each rescaling factor can be set arbitrarily, for instance to a value of 0.1.
3. Subtract each rescaled autofluorescence channel image from the BiFC channel image.
4. Examine the quality of the autofluorescence subtraction and repeat **steps 2** and **3** until a correct rescaling factor has been identified for each autofluorescence channel. The quality of the subtraction can be evaluated in several ways. Visual inspection of the subtracted image gives a qualitative impression of the efficiency of the subtraction and enables to readily identify a range of possible rescaling factors. To objectively fine tune each rescaling factor, it is possible to measure the mean and standard deviation of all pixel intensities in the subtracted image. A perfectly well-subtracted image should have a mean pixel intensity of zero. A positive mean indicates that a rescaling factor is too small, while a negative mean indicates that a rescaling factor is too large. In addition, the standard deviation

of pixel intensities in the entire image should be as low as possible and should be equal to the standard deviation of pixel intensities in background regions. Therefore, correct rescaling factors can be identified by minimizing both the absolute value of the mean and the standard deviation of all pixel intensities in the subtracted image.

5. Once each rescaling factor have been identified using images of no-BiFC control cells, they can be applied to subtract autofluorescence in other images acquired in identical conditions by repeating **steps 1–3** with these images.

3.3.4 BiFC Fluorescence and Cell Property Quantification

1. Open the subtracted BiFC fluorescence image.
2. Open the subcellular compartment mask produced in **step 8** of image segmentation. Multiply it with the subtracted BiFC fluorescence image. This produces an image where all pixel values are set to zero, except for pixels from the imaged subcellular compartment.
3. Open the mask produced in **step 9** of image segmentation. Multiply it with the subtracted BiFC fluorescence image. This produces an image where only the pixels corresponding to the imaged subcellular compartment are set to 0.
4. Open the binary image of the cells produced in **step 6** of image segmentation.
5. Perform a particle analysis in this image to define regions of interest (ROIs) corresponding to the cells that will be used in fluorescence quantification. Exclude cells that are touching the image edges or that are not circular. Set minimum and maximum pixel size areas to exclude too small cells and abnormally large cells or cell aggregates.
6. For each ROI, measure the integrated density in the image produced in **step 2** and divide it with the integrated density of the corresponding binary mask. This operation calculates the average BiFC fluorescence intensity in the subcellular compartment of each selected cell.
7. Repeat the operations described in **step 6** using the image produced in **step 3** and the corresponding binary mask. This calculates the BiFC fluorescence intensity in the rest of the cells.
8. Repeat **steps 1–7** with background subtracted images of the primary autofluorescence channel. This enables to identify cells that display an abnormally high or low fluorescence (e.g., as dead cells or out of focus cells, respectively) and to eliminate them in further analysis. It is also interesting to measure other cell properties such as size and shape parameters to be able to relate differences in BiFC intensities with different cell types.
9. To be able to compare BiFC fluorescence intensities measured in different experiments we recommend standardizing the

measured intensities such that BiFC signals measured in no-BiFC control cells have a mean of zero (which would be the case if background and autofluorescence subtraction were perfect) and a standard deviation of one. This operation is possible when a sufficient number of no-BiFC control cells are included in the analysis to precisely estimate these values.

10. Represent the standardized BiFC fluorescence intensities using a scientific graph plotting software.

4 Notes

1. To fully benefit from the capacity of BiFC to assay protein–protein interactions in near physiological conditions, we recommend performing BiFC experiments using cells that originate from the same organism as the investigated proteins. Still, it is possible to use BiFC in yeast to assay the interaction of heterologous proteins, as this is done for instance in yeast two hybrid assays. Plasmids that can be used to express heterologous proteins in yeast for BiFC experiments have for instance been described in [45].
2. BiFC images can be acquired with epifluorescence or confocal microscopes. In general, using a confocal microscope is not beneficial for yeast imaging, because there is no significant out-of-focus fluorescence [46]. Most protocols for live cell imaging of yeast therefore use epifluorescence (see for instance [47]). However, modern confocal microscope can be equipped with tunable band filters or spectral detectors. This offers a great flexibility in the selection of the emission passband and can be advantageous to define optimal BiFC imaging conditions and enable efficient autofluorescence subtraction. We currently perform our BiFC experiments using a Leica TCS SP8 confocal microscope.
3. Positive control strains are isogenic strains expressing fusion proteins known to produce a well-detectable BiFC signal (see for instance in [11]). They are used to verify the overall quality of the imaging procedure. no-BiFC control strains are isogenic strains that cannot produce any BiFC fluorescence, for instance strains that only express one of the two putative interaction partners. They are used to define parameters for autofluorescence subtraction, to verify its efficiency and to standardize the BiFC fluorescence measurements (*see* Subheading 3.3.4). no-BiFC control cells must be included in every BiFC experiment. They should not be confused with negative control strains that are isogenic strains designed to assay the specificity of PPIs detected by BiFC.
4. Many common laboratory strains (e.g., W303) are mutated in the *ADE2* gene. When grown in conventional YPD, these strains accumulate phosphoribosylaminoimidazole, an inter-

mediate in the adenine biosynthesis pathway, which is converted in the vacuole into a red pigment that strongly interferes with fluorescence microscopy. This can be minimized by supplementing the growth medium with 20 μg/mL extra adenine or by using ADE$^+$ strains (e.g., BY4741).

5. Protein folding and maturation of fluorescent proteins is temperature dependent [48]. Although Venus has been optimized for expression in mammalian cells at 37 °C, we observed that growing cells at 25 °C rather than 30 °C yields brighter BiFC fluorescence. Similar observations have been made with YFP [25, 49]. Performing the entire experiment at 20–25 °C also simplifies the imaging step since it is not necessary to use a microscope stage temperature controller.
6. To reduce yeast autofluorescence and avoid cell cycle synchronization it is best to keep cells actively growing (OD_{600} below 2) for several generations prior to imaging. To achieve this, overnight yeast cultures need to be inoculated at a low density so that they are not overgrown in the next morning. The exact OD_{600} at which the cultures are inoculated needs to be determined according to each strain generation time, which is ~2 h for wild-type haploid laboratory strains when cultivated at 25 °C.
7. Yeast imaging is performed in LFM medium [50], which does not contain riboflavin and folic acid and is therefore less autofluorescent than minimal media prepared from complete yeast nitrogen base (YPD is highly autofluorescent and must be avoided in fluorescence microscopy). Yeast should be cultivated in LFM medium a few hours prior to imaging.
8. In this protocol, yeast cells are imaged unattached, settled down on the glass cover slips. For best results, cells should be neither too scarce nor too dense. We suggest using a density of ~2×10^4 cells per square millimeter, which usually corresponds to ~2 μL of cells at an OD_{600} of 0.5. 8-Well chambers and 96-well plates have well surfaces of ~70 and ~30 mm^2, respectively.
9. The image processing procedure for autofluorescence subtraction described in this chapter works well if the autofluorescence channel images contain minimal bleed-through from BiFC fluorescence. If this is not the case, it is possible to perform a more sophisticated linear unmixing procedure which enables to separate and quantify overlapping fluorescence signals [51].
10. An example macro showing how the image processing steps described in this section can be automatized in ImageJ is available at https://github.com/grabut/BiFCanalysis
11. Several spatial filters can be used for image denoising. The Gaussian Blur and FFT Bandpass filters perform very well to remove pixel noise and small objects but they smooth edges. A

median filter better preserves edges. It is also possible to use more sophisticated algorithms such as anisotropic diffusion (http://fiji.sc/Anisotropic_Diffusion_2D) and non-local means filtering (http://fiji.sc/Non_Local_Means_Denoise).

12. Thresholding is a critical step in image processing as it strongly influences the final results. Initially, we suggest performing this step manually, using interactive selection of threshold values and visual inspection of the resulting binary images. However, when analyzing large series of images acquired under similar conditions, more robust results can be obtained using automatic thresholding procedures that are not affected by subjective selection of threshold values. Identification of a suitable automatic thresholding algorithm is not always easy. The Otsu and Mixture-of-Gaussian thresholding methods are commonly used in fluorescence microscopy.
13. Binary images produced by thresholding in ImageJ and Fiji have only two pixel values, 0 and 255, that represent black and white on an 8-bit scale. To be used as masks in image calculations, they need to be divided by 255 to have pixel values of 0 and 1. However, binary image operations and commands in ImageJ and Fiji (e.g., the "Analyze Particles") require binary images with pixel values of 0 and 255.
14. The background subtraction procedure described here assumes that the background intensity is evenly distributed in the imaging field. If this is not the case, more sophisticated procedures are required. For instance, if uneven background is due to uneven illumination, a flat-field correction should be applied [46].
15. In 32-bit float images, pixels can be assigned negative values, which is best for image processing and quantification (no pixel information is lost during background and autofluorescence subtraction).

Acknowledgements

This work received funding from the ANR (grant ANR-12-JSV8-0003-001) and Biosit. G.R. was supported by INSERM and E.B. received fellowships from the Ministère de la Recherche et de l'Enseignement Supérieur and La Ligue Contre le Cancer. Confocal microscopy was performed at the Microscopy Rennes Imaging Center (MRic) facility. The authors also would like to acknowledge networking support by the Proteostasis COST Action (BM1307).

References

1. Grabbe C, Husnjak K, Dikic I (2011) The spatial and temporal organization of ubiquitin networks. Nat Rev Mol Cell Biol 12:295–307
2. Rabut G (2012) Introduction to the pervasive role of ubiquitin-dependent protein degradation in cell regulation. Semin Cell Dev Biol 23:481
3. Clague MJ, Heride C, Urbé S (2015) The demographics of the ubiquitin system. Trends Cell Biol 25:417–426
4. Ye Y, Rape M (2009) Building ubiquitin chains: E2 enzymes at work. Nat Rev Mol Cell Biol 10:755–764
5. Li W, Bengtson MH, Ulbrich A et al (2008) Genome-wide and functional annotation of human E3 ubiquitin ligases identifies MULAN, a mitochondrial E3 that regulates the organelle's dynamics and signaling. PLoS One 3:e1487
6. Kulathu Y, Komander D (2012) Atypical ubiquitylation—the unexplored world of polyubiquitin beyond Lys48 and Lys63 linkages. Nat Rev Mol Cell Biol 13:508–523
7. Komander D, Rape M (2012) The ubiquitin code. Annu Rev Biochem 81:203–229
8. Markson G, Kiel C, Hyde R et al (2009) Analysis of the human E2 ubiquitin conjugating enzyme protein interaction network. Genome Res 19:1905–1911
9. van Wijk SJL, de Vries SJ, Kemmeren P et al (2009) A comprehensive framework of E2-RING E3 interactions of the human ubiquitin-proteasome system. Mol Syst Biol 5:295
10. Christensen DE, Brzovic PS, Klevit RE (2007) E2-BRCA1 RING interactions dictate synthesis of mono- or specific polyubiquitin chain linkages. Nat Struct Mol Biol 14:941–948
11. Khmelinskii A, Blaszczak E, Pantazopoulou M et al (2014) Protein quality control at the inner nuclear membrane. Nature 516:410–413
12. Kerppola TK (2008) Bimolecular fluorescence complementation: visualization of molecular interactions in living cells. In: Sullivan KF (ed) Methods in cell biology. Academic Press, New York, pp 431–470
13. Shyu YJ, Hu C-D (2008) Fluorescence complementation: an emerging tool for biological research. Trends Biotechnol 26:622–630
14. Kerppola TK (2009) Visualization of molecular interactions using bimolecular fluorescence complementation analysis: characteristics of protein fragment complementation. Chem Soc Rev 38:2876–2886
15. Kodama Y, Hu C-D (2012) Bimolecular fluorescence complementation (BiFC): a 5-year update and future perspectives. Biotechniques 53:285–298
16. Miller KE, Kim Y, Huh W-K et al (2015) Bimolecular fluorescence complementation (BiFC) analysis: advances and recent applications for genome-wide interaction studies. J Mol Biol 427:2039–2055
17. Kerppola TK (2013) Bimolecular fluorescence complementation (BiFC) analysis of protein interactions in live cells. Cold Spring Harb Protoc 2013:727–731
18. Weber-Boyvat M, Li S, Skarp K-P et al (2015) Bimolecular fluorescence complementation (BiFC) technique in yeast Saccharomyces cerevisiae and mammalian cells. Methods Mol Biol 1270:277–288
19. Schütze K, Harter K, Chaban C (2009) Bimolecular fluorescence complementation (BiFC) to study protein-protein interactions in living plant cells. Methods Mol Biol. 479:189–202. doi:10.1007/978-1-59745-289-2_12. PMID: 19083187
20. Morell M, Espargaró A, Avilés FX et al (2007) Detection of transient protein-protein interactions by bimolecular fluorescence complementation: the Abl-SH3 case. Proteomics 7:1023–1036
21. Magliery TJ, Wilson CGM, Pan W et al (2005) Detecting protein-protein interactions with a green fluorescent protein fragment reassembly trap: scope and mechanism. J Am Chem Soc 127:146–157
22. Kodama Y, Hu C-D (2010) An improved bimolecular fluorescence complementation assay with a high signal-to-noise ratio. Biotechniques 49:793–805
23. Levy ED, Kowarzyk J, Michnick SW (2014) High-resolution mapping of protein concentration reveals principles of proteome architecture and adaptation. Cell Rep 7:1333–1340
24. Ball DA, Lux MW, Adames NR et al (2014) Adaptive imaging cytometry to estimate parameters of gene networks models in systems and synthetic biology. PLoS One 9:e107087
25. Shyu YJ, Liu H, Deng X et al (2006) Identification of new fluorescent protein fragments for bimolecular fluorescence complementation analysis under physiological conditions. Biotechniques 40:61–66
26. Manderson EN, Malleshaiah M, Michnick SW (2008) A novel genetic screen implicates Elm1 in the inactivation of the yeast transcription factor SBF. PLoS One 3:e1500
27. Ohashi K, Kiuchi T, Shoji K et al (2012) Visualization of cofilin-actin and Ras-Raf interactions by bimolecular fluorescence complementation assays using a new pair of split Venus fragments. Biotechniques 52:45–50

28. Saka Y, Hagemann AI, Piepenburg O et al (2007) Nuclear accumulation of Smad complexes occurs only after the midblastula transition in Xenopus. Development 134:4209–4218
29. Nakagawa C, Inahata K, Nishimura S et al (2011) Improvement of a Venus-based bimolecular fluorescence complementation assay to visualize bFos-bJun interaction in living cells. Biosci Biotechnol Biochem 75:1399–1401
30. Lin J, Wang N, Li Y et al (2011) LEC-BiFC: a new method for rapid assay of protein interaction. Biotech Histochem 86:272–279
31. Sung M-K, Huh W-K (2007) Bimolecular fluorescence complementation analysis system for in vivo detection of protein-protein interaction in Saccharomyces cerevisiae. Yeast 24:767–775
32. Sung M-K, Lim G, Yi D-G et al (2013) Genome-wide bimolecular fluorescence complementation analysis of SUMO interactome in yeast. Genome Res 23:736–746
33. Salvat C, Wang G, Dastur A et al (2004) The -4 phenylalanine is required for substrate ubiquitination catalyzed by HECT ubiquitin ligases. J Biol Chem 279:18935–18943
34. Kühnle S, Mothes B, Matentzoglu K et al (2013) Role of the ubiquitin ligase E6AP/UBE3A in controlling levels of the synaptic protein Arc. Proc Natl Acad Sci U S A 110:8888–8893
35. Maspero E, Valentini E, Mari S et al (2013) Structure of a ubiquitin-loaded HECT ligase reveals the molecular basis for catalytic priming. Nat Struct Mol Biol 20:696–701
36. Huang L, Kinnucan E, Wang G et al (1999) Structure of an E6AP-UbcH7 complex: insights into ubiquitination by the E2-E3 enzyme cascade. Science 286:1321–1326
37. Kamadurai HB, Souphron J, Scott DC et al (2009) Insights into ubiquitin transfer cascades from a structure of a UbcH5B approximately ubiquitin-HECT(NEDD4L) complex. Mol Cell 36:1095–1102
38. Sommer T, Jentsch S (1993) A protein translocation defect linked to ubiquitin conjugation at the endoplasmic reticulum. Nature 365:176–179
39. Metzger MB, Liang Y-H, Das R et al (2013) A structurally unique E2-binding domain activates ubiquitination by the ERAD E2, Ubc7p, through multiple mechanisms. Mol Cell 50:516–527
40. Tong AHY, Boone C (2007) 16 High-throughput strain construction and systematic synthetic lethal screening in. In: Stansfield I, Stark MJR (eds) Methods in microbiology. Academic Press, New York, pp 369–707
41. Berndsen CE, Wolberger C (2014) New insights into ubiquitin E3 ligase mechanism. Nat Struct Mol Biol 21:301–307
42. Robida AM, Kerppola TK (2009) Bimolecular fluorescence complementation analysis of inducible protein interactions: effects of factors affecting protein folding on fluorescent protein fragment association. J Mol Biol 394:391–409
43. Blondel M, Bach S, Bamps S et al (2005) Degradation of Hof1 by SCF(Grr1) is important for actomyosin contraction during cytokinesis in yeast. EMBO J 24:1440–1452
44. Huang A, de Jong RN, Wienk H et al (2009) E2-c-Cbl recognition is necessary but not sufficient for ubiquitination activity. J Mol Biol 385:507–519
45. Malleshaiah MK, Shahrezaei V, Swain PS et al (2010) The scaffold protein Ste5 directly controls a switch-like mating decision in yeast. Nature 465:101–105
46. Waters JC (2009) Accuracy and precision in quantitative fluorescence microscopy. J Cell Biol 185:1135–1148
47. Rines DR, Thomann D, Dorn JF et al (2011) Live cell imaging of yeast. Cold Spring Harb Protoc 2011
48. Shaner NC, Steinbach PA, Tsien RY (2005) A guide to choosing fluorescent proteins. Nat Methods 2:905–909
49. Horstman A, Tonaco IAN, Boutilier K et al (2014) A cautionary note on the use of split-YFP/BiFC in plant protein-protein interaction studies. Int J Mol Sci 15:9628–9643
50. Sheff MA, Thorn KS (2004) Optimized cassettes for fluorescent protein tagging in Saccharomyces cerevisiae. Yeast 21:661–670
51. Zimmermann T (2005) Spectral imaging and linear unmixing in light microscopy. In: Microscopy techniques. Springer, Heidelberg, Berlin, pp 245–265
52. Luisier F, Vonesch C, Blu T et al (2010) Fast interscale wavelet denoising of Poisson-corrupted images. Signal Process 90:415–427